Rutherford Laboratory

~~64~~ 85

TECH/2/D.

Preprint

RPP/N-10

THE FAILURE OF NIMROD MAIN MAGNET POWER SUPPLY ALTERNATORS

by

H. C. BROOKS
(Rutherford High Energy Laboratory, England)

A. B. D. REED
(English Electric Co. Ltd., England)

RUTHERFORD HIGH ENERGY LABORATORY

CHILTON,

DIDCOT BERKS.

RPP/N-10

THE FAILURE OF NIMROD MAIN MAGNET POWER SUPPLY ALTERNATORS

by

H. C. BROOKS
(Rutherford High Energy Laboratory, England)

A. B. D. REED
(English Electric Co. Ltd., England)

A shortened version of this paper was presented at the U.S. National Particle Accelerator Conference 1-3 March, 1967, at Washington, D.C., U. S. A.

THE FAILURE OF NIMROD MAIN MAGNET POWER SUPPLY ALTERNATORS

by

H. C. BROOKS
Rutherford High Energy Laboratory, England

A. B. D. REED
English Electric Co. Ltd.,
England

SYNOPSIS

The paper describes the failure of one of the two magnet power supply alternators which resulted in the rewind of one stator and the modification and rebuild of the rotors of both alternators. This failure prevented Nimrod operating at 7 GeV from late February, 1965, to the end of November, 1965. Certain design changes made when the rotors were rebuilt are described. A resume is given of the investigations carried out immediately after the failure, while rebuilding was in progress, and after the machines were returned to service. Present plans are also briefly mentioned.

THE FAILURE OF NIMROD MAIN MAGNET POWER SUPPLY ALTERNATORS

1. Description of Installation
   Duty of Power Supply

2. Operational History up to Failure

3. Investigation of Failure
   - 3.1 Site examination
   - 3.2 Detailed examination of rotor
   - 3.3 Theoretical analysis

4. Modified Design

5. Experimental Investigations
   - 5.1 Laboratory Tests
   - 5.2 Site testing
     - 5.2.1 Resistance wire strain gauge measurements
     - 5.2.2 Use of piezo electric strain gauges
     - 5.2.3 Use of silicon piezo resistive strain gauges
   - 5.3 Site photoelastic investigation
     - 5.3.1 Work carried out on experimental rigs
     - 5.3.2 Work carried out on an alternator pole end plate under operational conditions
   - 5.4 Measurement of relative movement between key and end plate.

6. Analysis of Probable Causes of Failure

7. Present Policy

8. Acknowledgements

1. Description of Installation

Duty of Power Supply [1, 2, 3]

The synchrotron magnet has to be pulsed and at the commencement of each pulse 15 KV DC is applied to cause the current to rise from zero to 9,150 amps in 0.72 seconds. The energy stored in the magnetic field at this current is about 40 MJ. A typical magnet pulse is shown in Fig.1.

A power supply consisting of two 60 MVA 1,000 r/min motor-alternator-flywheel sets feeding transformers and mercury arc convertors is interposed between the magnet and the electricity supply network.

During the current rise period the machines act as generators, and at the beginning of flat top, half the convertors are switched from rectification to inversion, the remaining half following into inversion at the end of the flat top period. During decay time, energy is returned from the magnet to the machines which now operate as synchronous motors.

Fig.2 shows the circuit diagram of the power supply installation.
Fig.3 is an illustration of the rotating plant.
Figs. 4a and 4b show the machine duty during a pulse.

The pole construction as originally designed is shown in Fig.5

2. Operational History up to Failure

The first motor-alternator-flywheel set was installed and commissioned in conjunction with the convertor plant during the early part of 1962 and the power supply was used for a Nimrod magnet flux survey from May 1962 until August 1962.

The second set was installed during the latter half of 1962 and commissioning was completed during February 1963. Accelerator requirements were such that by the end of 1963 the number of magnet pulses was 1.75×10^6.

The accelerator continued in operation until 21st February, 1965, when a major failure occurred on No.1 alternator, which at this time had been subjected to about 7.25×10^6 pulses, many of these at less than 7 GeV.

On the evening of 21st February, 1965, a loud thud was heard from No.1 alternator and dense smoke emerged from it. The emergency trip was operated and, under braking, the set came to rest in fifteen minutes. The alternators were not energised at the time of the fault.

The rotating plant has vibration pick ups mounted on every bearing pedestal and shaft eccentricity pick ups are mounted adjacent to the alternator bearings. Fig.6 shows these locations and the alternator eccentricity and vibration recordings immediately before and after the fault occurred. It can be seen that all appeared to be very normal even seconds before the incident.

3. Investigation of Failure

3.1 Site examination of machine

The fault was caused by the failure of a rotor pole end plate across the neck region, (Fig.7), and the broken piece showed clearly the characteristics of fatigue failure (Fig.8). The stator was badly damaged and had to be rewound.

Repercussions on the shaft system had caused both drive motor rotors to rub on the stator laminations and minor damage had also occurred to fan casings.

All pedestals were examined for cracking and the end plates of No.2 alternator examined by ultrasonic and magnet crack detection techniques. Since these appeared to be sound it was decided to carry out strain gauge measurements in the neck region. Silver sliprings were used to feed the output from the strain gauges to a strain gauge amplifier and thence to a UV recorder.

Initially considerable difficulty was experienced due to slipring noise but nevertheless it was found that the stress distribution across the neck with the set at no load speed was as shown in Fig.9. It was also noticed that superimposed on the D.C. stress due to CF force was an alternating gravitational component of stress at rotational frequency having an approximate value of $\pm$ 1450 lbf/in^2 also shown on Fig.9.

At this stage the tests were stopped because a very small crack was detected in an end plate. This meant, unfortunately, that no tests under pulsing conditions could be carried out.

3.2 Detailed examination of rotor

Although the actual failure was very clearly due to fatigue, the cause was not apparent and a carefully planned programme of dismantling and examination was laid down. It was expected, and later proved to be the case, that the complete investigations would take many months. It was therefore necessary to record all observable details at each stage of examination before they were destroyed by further work. Many of the photographic records were of great value when the significance of certain factors became apparent during later investigations.

Examination of the fractured dovetail showed it to be a classical example of a fatigue failure with multiple starts, (Fig.8). The failure surface indicated several million cycles. The cracks had started on the side of the dovetail near the key corner, and had then propagated across about 75% of the section area before final tensile fracture occurred. Four other end plates of the failed rotor were found to have cracks in an earlier stage of development. One of these end plates clearly showed the multiple starts to the cracking (Fig.10). It was interesting to note that all failures, except one, appeared to be at the flywheel end, where the large shaft torque changes occur. Examination of the various cracks suggested that they all started in the area A, B, C of Fig.5. There was little evidence of a preferred side for the crack to start. This suggested that tensile and transverse bending stresses could be significant.

The pole side of the keys showed that laminated portions of the pole were well bedded against the key surface, with little sign of fretting or pick up. In the region of the end plate there was evidence of fretting especially on the top edge of the key. Fretting had occurred particularly between key and end plate, rather than between key and rotor body.

The shafts were examined in great detail by ultrasonic, dye penetrant and magnetic crack detection methods and were found to be free of cracks, and suitable for further service.

A sample of the pole laminations was examined. This showed

that away from end plate failure zones, all laminations were likely to be sound. Laminations adjacent to end plates in which advanced cracks were present, usually contained fractures which arose from redistribution of load as the end plate crack advanced.

3.3 Theoretical Analysis

The dovetail fixing had been considered during the initial design and account taken of the variable loads and of the stress concentration factors (S.C.F.), the latter being estimated as 1.7 and obtained from photoelastic tests. The reasons for failure were therefore not readily apparent. As a first step operating conditions were carefully re-examined. This was the first known failure of a dovetail pole fixing under design service conditions, and this strongly suggested the failure was associated with the particular duty. Two fields were investigated:

(i) Additional forms of loading which could be significant.

(ii) Examination of the known loadings to determine whether they acted in a different manner to that anticipated in the original design.

3.3.1 Additional loadings

Several aspects were considered. It was found that both rotors had been subjected to the effects of many more rectifier backfires than anticipated and the set with the broken end plate had experienced the larger number. However, examination showed that there were inconsistencies in respect of both load and number of cycles. It was therefore considered that this was not a cause of failure, although it could accelerate the rate of damage. The effects of flux changes were reconsidered and the original design levels confirmed. The dynamics of the complex pole-shaft-flywheel system structure were analysed. It was found that the torque loads could be up to 20% higher on the flywheel end. While this might explain the tendency for the end plates at the flywheel end to fail first, this phenomenon was not very significant. Various other effects were studied. For example, thermal stresses produced by excitation trips were investigated but it was concluded that although these

aggravated the loading condition, they were not likely to cause failure.

3.3.2 Alternative mechanisms for known loading

Consideration was given to the neck stresses including those due to key compression. The significant loads on the dovetail neck are due to centrifugal force, torque and gravity. It was known that, at speed, the underside of the pole no longer remained in contact with the rotor body.

The centrifugal loadings on the end plate arise from its own mass, and that of the part of the rotor coil which it supports. From Fig.5 it will be seen that the end turns are supported on a projecting lip on the plate. At the original design stage it was considered that this eccentric load was resisted by the laminations and that the end plate was able to take up the appropriate attitude. However, if the dovetail is restrained and the support offered by the laminations small (i.e. the pole is loosely consolidated) then considerable bending moments can be produced about the axis X-X (See Table I and Fig.5). Close examination and measurements on the poles showed that such a mode of behaviour was indeed possible even with normal consolidation.

During a standard pulse (see Ref.1) the speed varies by $\pm 2.1\%$ thus giving a stress variation of $\pm 4.2\%$. This variation would be superimposed on the direct and bending components.

During the testing of the second alternator (Section 3.1) it will be remembered that a gravitational (rotational frequency) variable stress component was seen, but the full significance of this result was not immediately appreciated. The effects of gravity on the pole stresses had been examined but the variable stress on the neck due to the self weight of the pole was small. However, it acts in a more subtle way. Due to the sag of the shaft there is a very small angle ϵ Fig.11 between the catenary line at the end plate and the axis A B. This means that the effective pole length oscillates between C D and E F producing changes in lamination

pressure and a resulting rotational frequency bending about the X X axis (Fig.5). This stress is very difficult to estimate with any certainty. Nevertheless calculated and measured values showed reasonably close agreement. This stress variation is a feature of all horizontal machines of keyed laminated pole construction.

Reference to Table I shows that without stress concentration it was estimated that the mean direct tensile stress across the neck was in the range 31-39,000 lbf/in^2 upon which was superimposed a variable component of 3,400-4,200 lbf/in^2. The make up of these stresses is shown in Fig.12.

Even after allowing for SCF of 1.7 (based on the nominal neck stress) a Goodman diagram for the conditions showed the end plate to be well removed from failure.

It was clear that a fundamental discrepancy existed.

Loads high enough to institute failure did not seem to be present and therefore interest was centred on the local conditions between the key and pole dovetail. The situation had features in common with those recently discovered after failures of steam turbine shafts at low variable stresses[8]. These were:

(i) The key and pole are held in contact under high compressive stresses and could behave as solid material.

(ii) In such a configuration as in (i) then the transition between dovetail neck and key represents a very sharp corner. Material in this corner is subject to high tensile stresses.

If strength reduction factors comparable with those found in the turbine investigation were applicable, then the margins were very significantly reduced. The strength reduction factor is the ratio of the fatigue strength of the material at zero mean stress with no stress concentration present, to the fatigue strength achieved by the material in

an actual configuration.

The other factor which appeared to be important was fretting. Some of the cracks in the end plates had propagated in the areas of fretting damage at the top corner of the key. Fretting has been recognised for many years, but only in more recent years has it been appreciated that such large strength reduction factors may exist with particular circumstances and materials. It is difficult to apply the present knowledge quantitatively to the situation, but it was found that the right conditions existed for fretting fatigue damage to occur. The torsion of the shaft and the small changes of centrifugal loading could both produce the required oscillatory movement. Because the major torque pulsations occur at the flywheel end it is possible the small movements associated with these increase fretting at this end and hence risk of failure. The necessary pressure is inherent in the arrangement. Further theoretical analysis of this aspect was difficult and experimental work was essential.

At this stage it appeared that each of the supposed mechanisms could not alone produce failure, but in combination could well do so.

4. Modified Design

It was essential to have the proton synchrotron operational again in the shortest possible time. A decision to radically redesign the rotors involving new forgings would have meant up to two years delay and so it was decided that provided worthwhile improvements could be made, the existing rotor forgings and pole laminations should be used again. With this policy it was clear that there were strict limits on permissible changes and that the basic keyed pole construction was implied.

It must also be remembered that these decisions had to be made well before any of the extensive theoretical and laboratory investigations were completed. The complete investigation might show that a modified rotor had only limited life, but there was sufficient confidence that a real improvement could be achieved, to justify this course of action.

The following modifications were made:-

4.1 The end plate material was changed to a high strength forging to give a gain of 50% to 60% in nominal properties. The only high strength forging materials readily available which would develop good properties in the heavy sections were high alloy steels, and of these 2½% Ni-Cr-Mo was considered most suitable. In these more specialised materials delivery can be a problem and none of this was immediately available. Fortunately a forge was found which had 12,000 lb. of acceptable 1½% Ni-Cr-Mo steel of the right size for forging into end plates, and work was commenced immediately on the first set. For forgings on the second rotor 2½% Ni-Cr-Mo was used on account of its better ability to develop the required properties in heavy sections. The forgings were arranged to obtain good grain flow in the critical neck region. After rough machining the forgings were heat-treated to develop a yield strength of 110,000 lbf/in^2.

4.2 To reduce the general level of neck stresses the neck thickness was increased from 5 inches to 6 inches.

4.3 If either fretting or stress concentration was significant in the failure then steps were necessary to modify the dovetail end plate and lamination geometry. The change is shown in Figs. 13a and 13b. If under the high loads the assembly behaved as solid material, there was a smooth transition between neck and key somewhat reducing any stress concentrations in the tensile fibres. If fretting was a contributing factor to failure then it would occur at point A, but since this was now considered to be in a region of reduced tensile stress the possibility of crack formation and propagation was reduced. Further down the key-pole interface the conditions of fretting and tensile stress very rapidly improve and failure here was extremely unlikely. It was not possible to provide an ideal transition radius normal to the bedding face, due to strength restrictions on the remaining dovetail section (Fig.13b). Additionally the key was extended axially past the pole.

4.4 The machining processes on the end plate were arranged

as far as possible for any machining marks to lie parallel to the neck axes, thus giving the best fatigue resistance. The stressed areas were finished by polishing to about 16 micro inch finish.

4.5 To minimise any bending stresses due to the overhung copper the laminations were consolidated during pole construction to three times the original pressure and retained by higher tensile tie rods.

4.6 Close attention was paid to the quality of the bedding between keys and pole, especially in the region of the end plate to ensure the conditions necessary for 4.3 were attained.

4.7 A phosphate/molybdenum disulphide treatment was applied to the keys since it was considered that this would be beneficial in reducing the extent of fretting and corrosion and hence the risk of crack initiation on the pole faces.

4.8 The location of rotor excitation connections was altered in order to allow access to the end plates for ultrasonic examination.

Part of the complete new pole, prior to assembly on the shaft, is shown in Fig.14.

5. Experimental Investigations

5.1 Laboratory Tests

It was clear from the initial theoretical work that many factors could have contributed to failure, and exact assessment of these was difficult without experimental evidence. The changes in the design were therefore euqally difficult to justify and it was by no means certain that these changes would be completely effective. Accelerated laboratory testing was considered to be a valuable guide. A comprehensive test programme was therefore designed to investigate the fatigue behaviour of end plates.

The aims were:

(i) To verify that the actual failures could be reproduced in a laboratory rig by loads which were postulated as the cause of failure.

(ii) To investigate the effect of changes of dovetail geometry and material and hence assess the performance of a modified design.

A rig was therefore designed (Fig.15) to accept a full sized section of end plate but of reduced thickness. The actual loading in the rotor is a complex combination of pulsating direct loads, and bending stresses in two planes. Any attempt to reproduce this exactly would be impracticable. The loading system was therefore simplified to represent the cross section with the highest stress, i.e. the outer surface of the end plate. A steady tensile load was applied by a hydraulic jack, and the variable direct and bending stresses were produced by a rotating out-of-balance weight attached to the test specimen at an appropriate point. In addition to fatigue tests the rig was used to investigate dynamic and static behaviour of the dovetail arrangement and for photoelastic coating investigations.

The first step was to attempt to reproduce the conditions of the failure. Tests were carried out at a mean nominal stress of 43,500 lbf/in^2. The cyclic stress component was varied from $\pm$19,500 lbf/in^2 to $\pm$4,000 lbf/in^2 over 8 unrelieved cast end plate specimens and the results of these runs gave a stress-life curve, (Fig.16), which was acceptably consistent with the failure. Additionally the mode of failure on the specimens was very similar to that on the actual machine.

A satisfactory basis having been established it was now possible to evaluate the rotor dovetail modifications. As already mentioned in order to restore the rotor in the minimum possible time, a decision on the design modifications had been taken on the basis of a design assessment of the failure and that this subsequent test programme could only confirm or reject the design basis. This was a risk which was accepted.

The main changes concerned a material change to forged steel and a geometry change in the form of a relieved keying surface. To evaluate these, cast steel specimens with relief, and forged steel specimens with and without relief were prepared. A test programme along similar lines to the original was laid down for each.

The first results from the "relieved" cast steel specimens were at first sight surprising since the relief did not give any significant improvement in the fatigue life. This caused serious doubt to be placed on the redesigned rotor which was in an advanced stage of manufacture.

The unrelieved forged specimens gave very little change in life but the effect of the relief on this material was startling - it was very difficult to obtain a fracture at all. Fractures were eventually obtained by making specially reduced thickness specimens in which much higher stresses could be induced by the rig. It was found the fatigue limit was equivalent to $\pm$29,000 lbf/in^2 for the new end plates compared with about $\pm$4,500 lbf/in^2 for the original end plates, both at the same steady stress level. It should be noted that the curves shown in Fig.16 do not quite match these levels, as the properties of the forged test specimens were lower than those actually used.

With this vindication of the redesigned dovetail, tests were continued to ensure that no mechanism (such as fretting) would become significant after a large number of cycles. Two test runs were extended to 10^8 cycles at stresses above operating conditions without any sign of distress.

It was thus established that the performance of the redesign represented a major improvement over the original.

The original pole body laminations were being re-used (albeit with the keying face relieved) and samples of these were tested with appropriate loadings in this rig with completely satisfactory results.

5.2 Site Testing

5.2.1 Resistance wire strain gauge measurements

During assembly at the manufacturer's works resistance wire strain gauges were installed on the side faces of several end plates and after re-assembly on site additional ones were installed on the front faces. Fig.9 shows a typical arrangement, together with stress distributions

obtained. It also indicates that pole to pole variation has the order of consistency one would expect. These curves were obtained with the set at speed but not pulsing.

It was interesting to note that gauges positioned perpendicularly to the keys indicated signs of pole settling at the onset of initial pulsing. For example an early test at speed but not pulsing on an F3 gauge on one of the poles gave a compressive reading of 65,000 lbf/in^2 but after pulsing had reduced to a value of 36,000 lbf/in^2. Furthermore the range of stress variation of the F gauges had been reduced.

Stress recordings when pulsing proved difficult to evaluate due to high noise levels. Noise level from the special strain gauge slipring assemblies used was reduced to an acceptable level but electrical noise levels due primarily to the gauge locations within the machine remained a problem.

Nevertheless, analysis of cyclic stresses from the recordings obtained was carried out and results showed a mean stress of 26,000 lbf/in^2 $\pm$2,200 lbf/in^2. This shows reasonable agreement with the estimated stresses shown in Table I. However, it was considered possible that some fast stress overshoots might occur particularly at torque change periods due, for example, to pole mechanical resonance effects. Any such effects as these were masked by the high noise level.

The use of contactless telemetering systems was considered but rejected for two principal reasons:-

(1) development and setting up of existing commercial equipments for this particular application would have taken too long, and

(2) experience seemed to indicate that the mode of alternator operation would still have caused serious interference problems.

5.2.2 Use of Piezo electric strain gauges

Lead zirconate crystals were tried. These, of course, do not respond to steady state conditions and when measuring cyclic stresses it is advantageous to feed the crystal into a much higher impedance circuit than that represented by the strain gauge wiring and sliprings. This is particularly important at very low frequencies and Nimrod pulsing frequency is of the order of 0.5 cycle per second.

The gravitational component of stress when the machine is running at a constant no load speed as shown in Fig.9 was clearly observed however. This suggests that any excess stresses at rapid torque change periods (beginning and end of flat top) should have been apparent, as should any stresses due to mechanical resonance effects. No such excess stress levels were observed.

5.2.3 Use of silicon Piezo resistive strain gauges[4]

Semi conductor strain gauges have strain sensitivities almost one hundred times greater than conventional resistance wire gauges. Strain-resistance relationship of such a gauge is non linear, and, furthermore temperature changes induce changes in resistance and in strain sensitivity. It was fortunate that in our application accuracies within $\pm 10\%$ were acceptable and reference to Fig.17 will indicate that over the range of stresses and temperature in which we were interested it was not necessary to take any special precautions.

Fig.18 shows typical results obtained and once again no excess cyclic stresses were observed. The form of stress make-up shown in Fig.12 is seen to be generally confirmed. Again the gravitational component of stress as shown in Fig.9 can be seen.

5.3 Site photoelastic investigation[6]

5.3.1 Work carried out on experimental rigs

Investigation using a test rig similar to that described

in Section 5.1 confirmed that the stress concentration factor across the narrow neck section is about 1.7 but in the 5/8" radiused neck edge region it was found to be 1.9 ±0.2 for the new design and 2.15 ±0.2 for the old design. As before the concentration factor is based on the nominal stress in the minimum neck section.

It was also found that on the new design the very localised region of maximum tensile stress occurred about 2/3 of the way round the 5/8" radius away from the key, whereas in the old design the distance of the highest tensile stress was only about half this distance away from the key.

Static model results suggest somewhat higher compressive stresses in the new design in the key region.

5.3.2 Work carried out on an alternator pole end plate under operational conditions

Photoelastic material was cemented to a pole end plate on the alternator and techniques were developed to enable still and cine photography to be carried out when the machine was pulsing. The highest stress observed in the neck region immediately above the thick key section was 55,000 lbf/in^2 ±6,700 lbf/in^2. Only 41,500 lbf/in^2 ±4,500 lbf/in^2 was observed in the neck region just above the thin key section. It was not easy to evaluate the cyclic stress components since the cyclic stresses in this case represent only about 0.25 to 0.3 of a colour fringe. With a stress concentration factor of 2 applied it will be noted that these figures are in close agreement with Table I.

Compressive stresses in the pole end plate immediately adjacent to the thick key region were observed to be of the order of 72,000 lbf/in^2.

5.4 Measurement of relative movement between key and end plate

A limited amount of work has been carried out to enable measurements to be made of the relative movement between the pole end plate

and the key. An inductive transducer was screwed into an aluminium block which was then cemented to an end plate. A second aluminium block containing a steel anvil was cemented to the key. The arrangement is shown in Fig.19a.

The transducer used was of the double variety so that one transducer could be used as a temperature compensating dummy while the other was used for the displacement measurement[5]. The block diagram of the circuit used is shown in Fig.19b. The transducers formed two arms of a bridge; the other two arms were inside the amplifier and were adjusted to balance the bridge. The bridge was fed with a 30 volts peak to peak signal at 50 K c/s and under these conditions a sensitivity of 20 mV per 0.001" of movement was obtained. The amplifier increased this sensitivity to 200 mV per 0.001" of movement.

When the machine was run up to speed a displacement between key and end plate of 0.004" was observed. As the machine was shut down the key and end plate resumed their zero speed position.

Fig.19c shows various key movements recorded under a variety of pulsing conditions.

It is interesting to note that these preliminary results suggested that with longer flat top settings the total displacement was reduced. It is frequently held that the most serious frettage attacks which tend to lead to cracking occur when the relative displacements of the two surfaces in question are in the region 0.0002" - 0.002". With larger amplitudes of movement the surfaces often wear rather than crack. Relative movements of key and end plate assembly on the present machines appear to be in this critical range under pulsing conditions.

6. Analysis of Probable Causes of Failure

A good insight into the probable causes of failure is obtained from the experimental investigations. These show that all the mechanisms postulated in Section 3.3.2 are present. The relative importance of the factors is a function of geometry and material and the effectiveness of any design may be expressed in terms of a strength reduction factor. The results show that in the original design, crack initiation could

occur due to either fretting or conventional fatigue, the stresses necessary to cause this being of similar order of magnitude. The reduction of the fretting phenomena by having a relieved profile on the cast specimens produced little improvement, i.e. there was still an appreciable strength reduction factor applicable. The unrelieved forged specimens failed by fretting-fatigue. Once any crack is formed the higher mechanical strength of this material is not fully realised because of notch sensitivity. There is therefore little improvement on the original situation. With the removal of the fretting situation to a "safer" area by provision of the relief, the improved properties of the forging are now utilised, and additionally the strength reduction factor is lower than that of the casting. With the reduction of stresses in the new design and the improved strength of the arrangement it is estimated that on the basis of variable load levels the design is improved by a factor approaching 10.

It is concluded that the failure was due to a combination of three factors, each of which acting alone would not have produced failure. These factors were:

(i) The precise mechanism by which the stress summation at certain critical points was aggravated by the pulsing duty was not fully appreciated.

(ii) The geometry and material were such that a large strength reduction factor was obtained.

(iii) Fretting occurred in a critical region.

7. Present Policy

The rebuilt rotors have now been subjected to 9.0×10^6 7 GeV pulses and the end plates are examined ultrasonically about every 1.5×10^6 pulses. Special probes have been developed to work in conjunction with certain units of the ultrasonic equipment developed to monitor the Nimrod rotors[7]. In order to separate the twin motor alternator flywheel shaft systems, the alternators are now operated in parallel with the shaft coupling between the two flywheels disconnected.

Investigations are still proceeding to:-

(1) evaluate yet more clearly the cyclic stresses acting on the end plates,

(2) determine whether photoelastic techniques are likely to give earlier warning of cracking than the ultrasonic techniques at present in use and,

(3) obtain more information about rotor key movement. Measurements so far made have been carried out on only one end plate.

Such investigations tend to be very protracted because accelerator operational and development requirements limit the opportunity to conduct tests on the alternator to a few hours per month.

The interplay of all the forces acting on the rotor is very complex and the mechanism of fretting fatigue is not perfectly understood. On any keyed form of pole construction relative movement must occur within such keyed assemblies. It was therefore considered prudent to order a spare rotor having solid poles forged integrally with the body, although it is realised that in this form of construction problems can arise in the pole shoe to pole body assembly regions.

The possibility of replacing the complete rotating plant by a saturable reactor network compensation device which would enable 7 GeV pulsing direct from the electricity supply network is also being reviewed[9, 10].

8. Acknowledgements

The work described in this paper was the result of a sustained combined effort on the part of a large number of people at the Rutherford High Energy Laboratory, the English Electric Co. Ltd., and Lloyds Register of Shipping. The authors would particularly stress the extent of their colleagues' contribution and find it difficult to single out names.

Nevertheless they feel they must specifically acknowledge the contributions made by Dr. H. H. Atkinson and Mr. A. J. Middleton of R.H.E.L. and Messrs. I. E. McShane and P. G. Morton of E.E.Co.Ltd.

The authors also wish to acknowledge the permission given by their respective organisations to publish this paper.

REFERENCES

1. BOWLES, P., HADLEY, H., and MARCHBANKS, M. J. :
'Magnet power supply for the 7 GeV proton synchrotron Nimrod'.
Part 1 General. Proceedings I.E.E., Vol.110, No.3, March 1963,
pp. 561-572.

2. FOX, J. A., TAYLOR, D. G., and WILSON, R. :
'Magnet power supply for the 7 GeV proton synchrotron Nimrod'.
Part 2 Rotating machines. Proceedings I.E.E., Vol.110, No.3,
March 1963, pp. 573-590.

3. ROLLIG, K., and HODLE, H. :
'Magnet power supply for the 7 GeV proton synchrotron Nimrod'.
Part 3 Mercury-arc convertors. Proceedings I.E.E., Vol.110,
No.3, March 1963, pp. 591-602.

4. HIGSON, G. R. :
'Recent advances in strain gauges'.
Journal of Scientific Instruments. Vol.41, July 1964, pp. 405-414.

5. WESTBROOK, M. H., MUNRO, R. :
'Electronic Instrumentation Techniques in the Development of
Pistons and Rings'. I. Mech. E. Symposium on 'The Accuracy of
Electronic Measurements in internal combustion engine develop-
ments'.
Proceedings I. Mech. E. 1965/66 Vol.180, Part 3g, Paper 6.

6. ATKINSON, H. H., HYMAN, J. T., MALTON, R. W., STARLING, P. P.
'Photoelastic Investigation of Stress in Nimrod Alternator Pole
End Plates'. (In course of preparation at Rutherford High Energy
Laboratory).

7. BROOKS, H. C., BROWN, A. W., RANKIN, A.C. :
'Ultrasonic Inspection of the Nimrod Power Plant Alternator Rotors'.
Proceedings of the Fourth International Conference on Non Destructive
Testing, pp. 196-202.

8. COYLE, M. B., WATSON, S. J. :
'Fatigue Strength of Turbine Shafts with Shrunk-on Discs'.
Proceedings I. Mech. E., 1963-4, pp. 147-179.

9. FRIEDLANDER, E. :
'Static network stabilisation. Recent progress in Reactive Power
Control'. G.E.C. Journal of Science and Technology. Vol.33,
No.2, 1966.

10. FOX, J. A. :
'A static power supply for the 300 GeV Accelerator Magnet System'.
Rutherford High Energy Laboratory Publication Ref.E/PS-DS/300 GeV/JAF-1.

TABLE AND ILLUSTRATIONS

Table I	Estimated endplate stresses
Fig.1	Simplified pulse waveforms of magnet current and voltage
Fig.2	Nimrod power plant schematic diagram
Fig.3	Motor-alternator-flywheel sets
Fig.4	Simplified characteristics showing alternator loading during a typical pulse
Fig.5	Original pole construction
Fig.6	Shaft eccentricity and vibration
Fig.7	Damaged pole and stator
Fig.8	Lower half of fractured dovetail
Fig.9	Strain gauge locations and measurements
Fig.10	Cracked endplate
Fig.11	Shaft stress catenary effect
Fig.12	Stress variations (simplified) during a pulse
Fig.13	Pole dovetail profiles
Fig.14	Part of re-designed endplate pole assembly showing reliefs
Fig.15	Test rig for endplate profile and material evaluation
Fig.16	Fatigue curves obtained from test rig results
Fig.17	Silicon piezo resistive strain gauge characteristics
Fig.18	U.V. recordings of cyclic stresses using piezo resistive strain gauges
Fig.19	Measurement of key/endplate movement

TABLE I Estimated End Plate Stresses

Stress Components	Mean Tensile Direct	Tensile Transverse Bending	Tensile Longitudinal Bending *	Design
Due to lamination clamping pressure			−1700 to −3400	OLD Mean stress is therefore 39600 max to 31200 min Alternating stress is ±4240 max to ±3450 min
Centrifugal (950 r/min)	+24000		+11200 to +17900	
Due to speed change (P.R.F. -approx. 0·5 c/s at 7GeV)	± 1000		± 470 to ± 760	
Due to gravitational effect (approx. 16 c/s)	± 30	± 390	±1300 to ±1800	
Due to load torque (P.R.F. - approx. 0·5 c/s at 7GeV)		± 1200		
Due to shaft torsional oscillation (approx. 20·4 c/s)		± 1000		
Due to lamination clamping pressure			− 2700 to −4000	NEW Mean stress is therefore 31650 max to 24950 min Alternating stress is ± 3130 max to ± 2680 min
Centrifugal (950 r/min)	+24000		+ 5600 to +17000	
Due to speed change (P.R.F. -approx. 0·5 c/s at 7GeV)	± 1000		± 220 to ± 470	
Due to gravitational effect (approx. 16 c/s)	± 30	±400	±670 to ±900	
Due to load torque (P.R.F. -approx. 0·5 c/s at 7GeV)		± 1300		
Due to shaft torsional oscillation (approx. 20·4 c/s)		± 1100		

Key
± Alternating stresses
− Compressive stresses
+ Tensile stresses

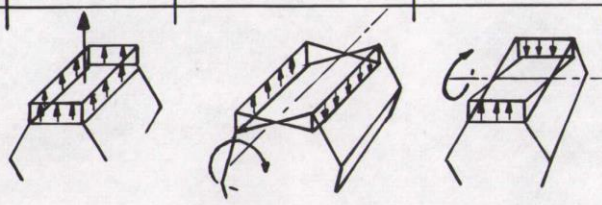

All figures in lbf/in² & not inclusive of stress concentration factors. The figures are for 7GeV operation with a speed variation of 40 r/min.

Note *
Estimates for longitudinal bending stresses have a wide range dependent upon assumptions made concerning support given by laminations, friction, dovetail fixing characteristics etc.

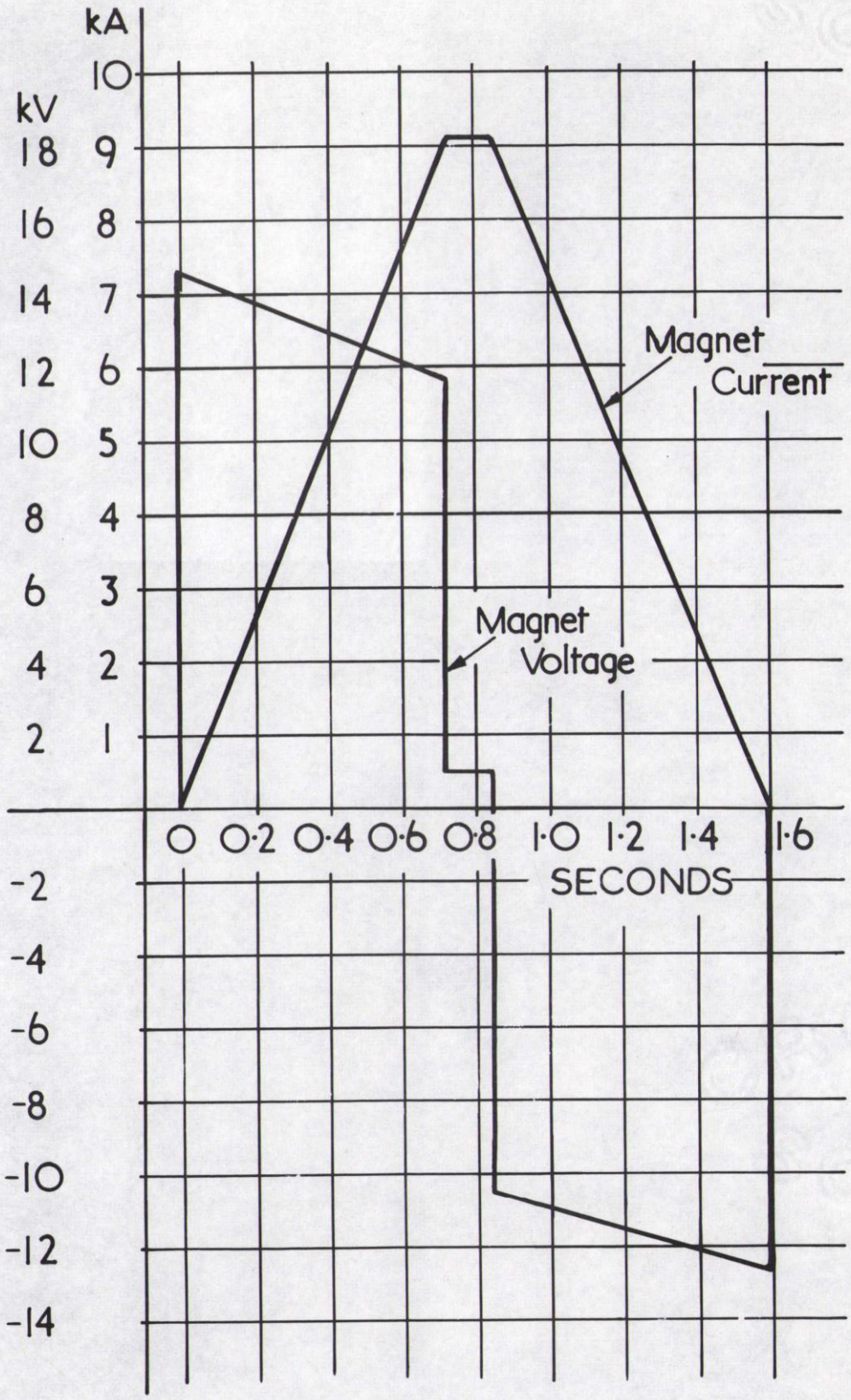

FIG. 1 SIMPLIFIED PULSE WAVEFORMS OF MAGNET CURRENT & VOLTAGE

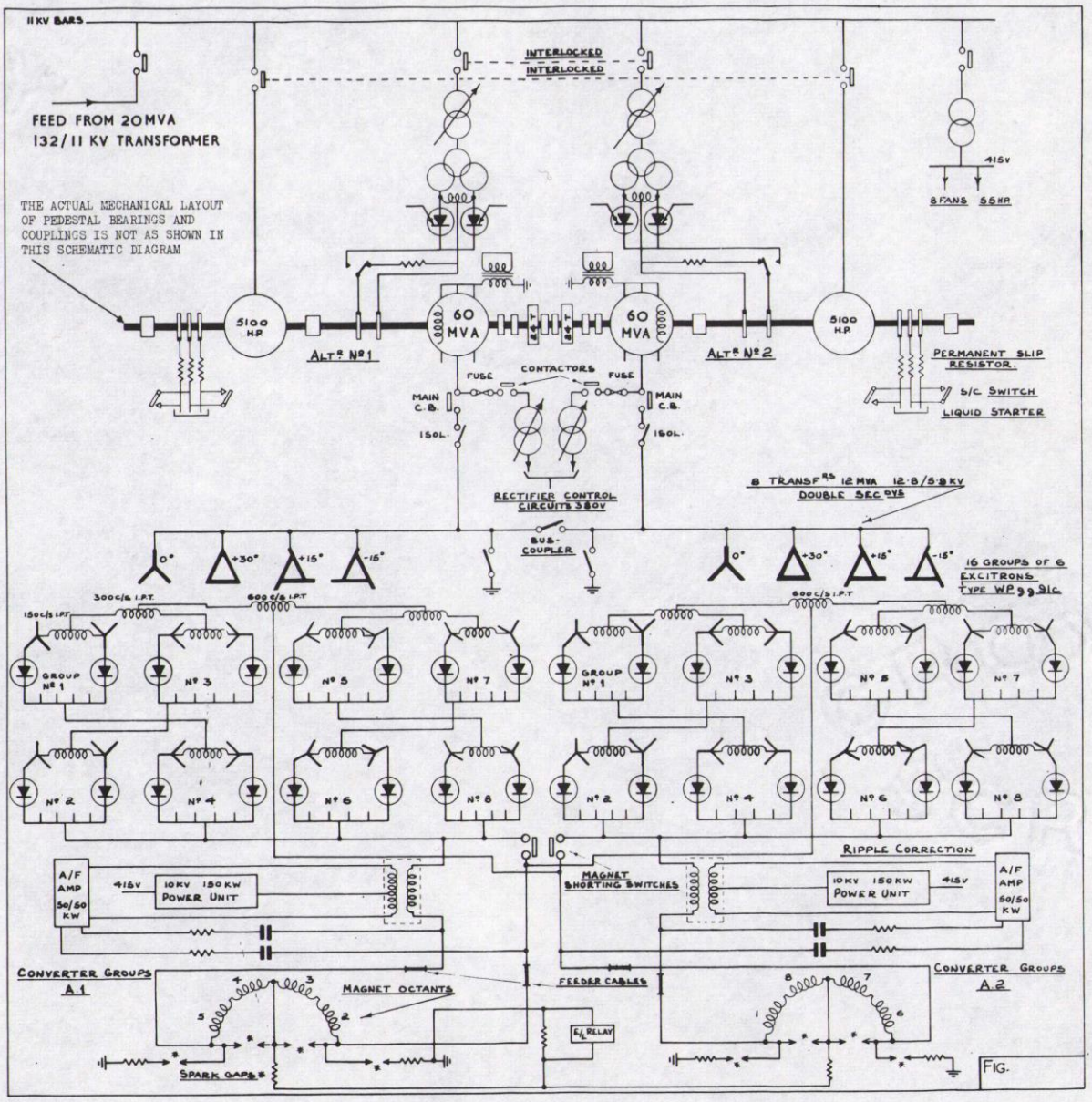

Fig. 2 Nimrod Power Plant Schematic Diagram.

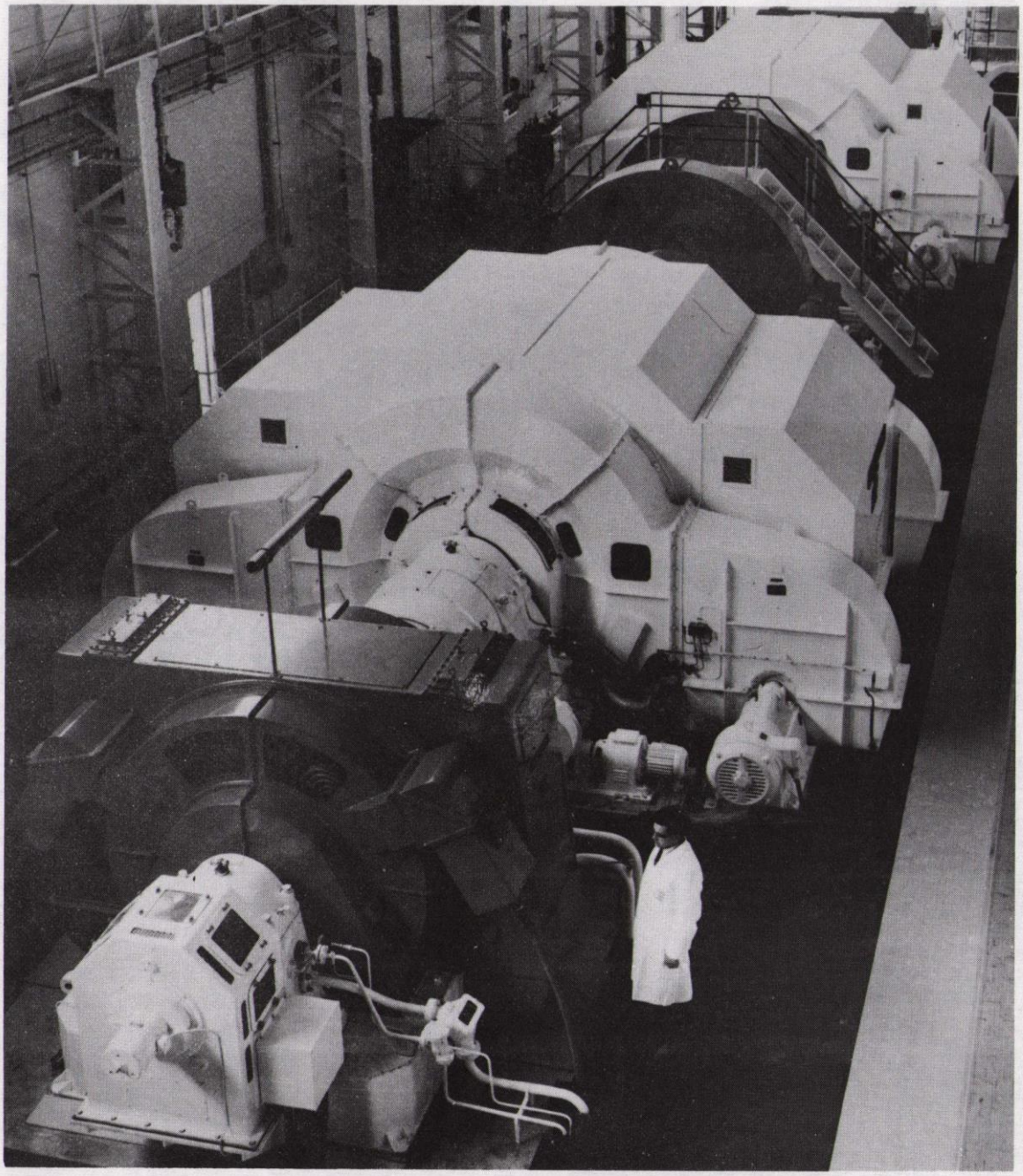

FIG.3 MOTOR-ALTERNATOR-FLYWHEEL SETS

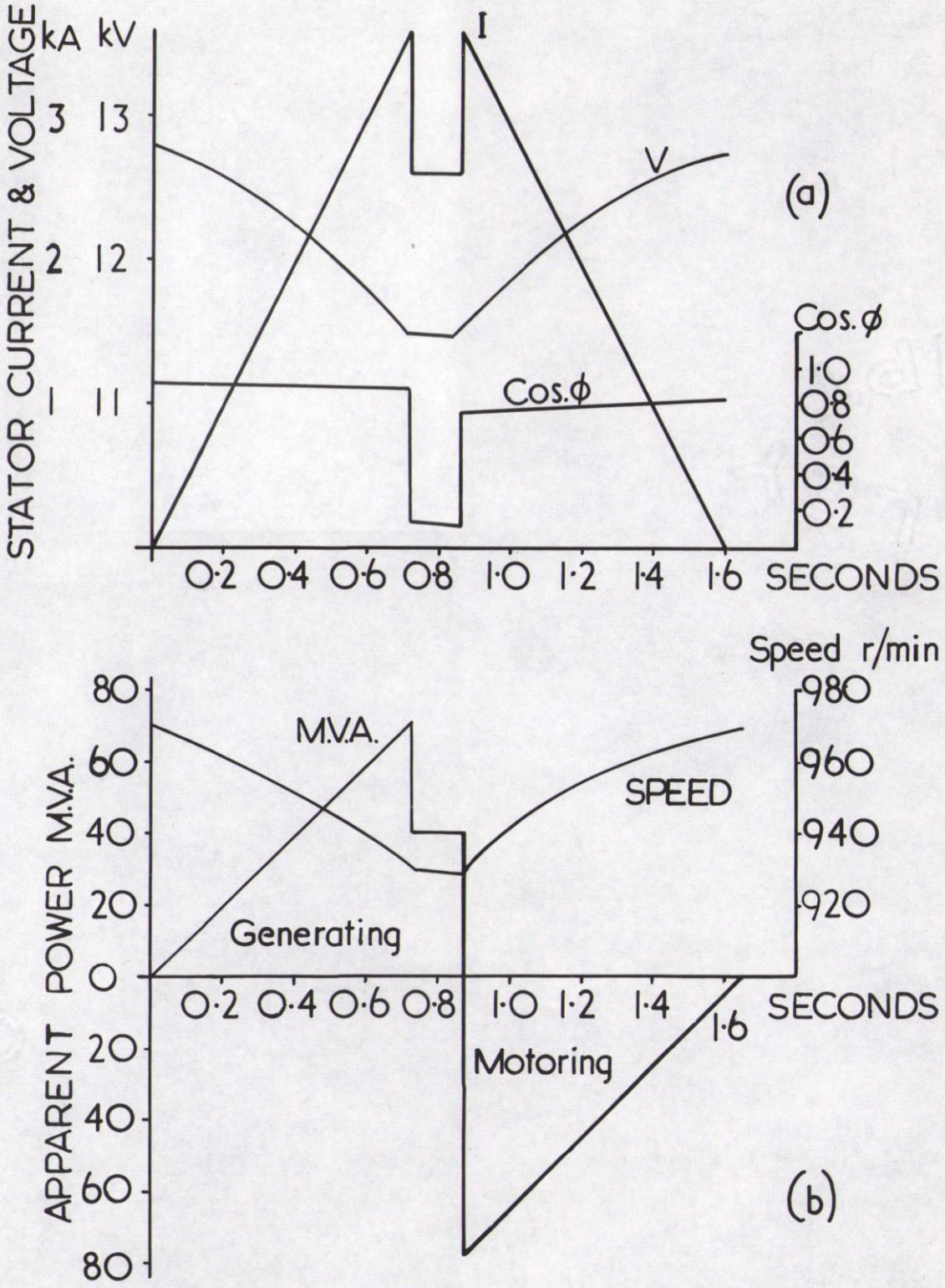

FIG. 4 SIMPLIFIED CHARACTERISTICS SHOWING ALTERNATOR LOADING DURING A TYPICAL PULSE

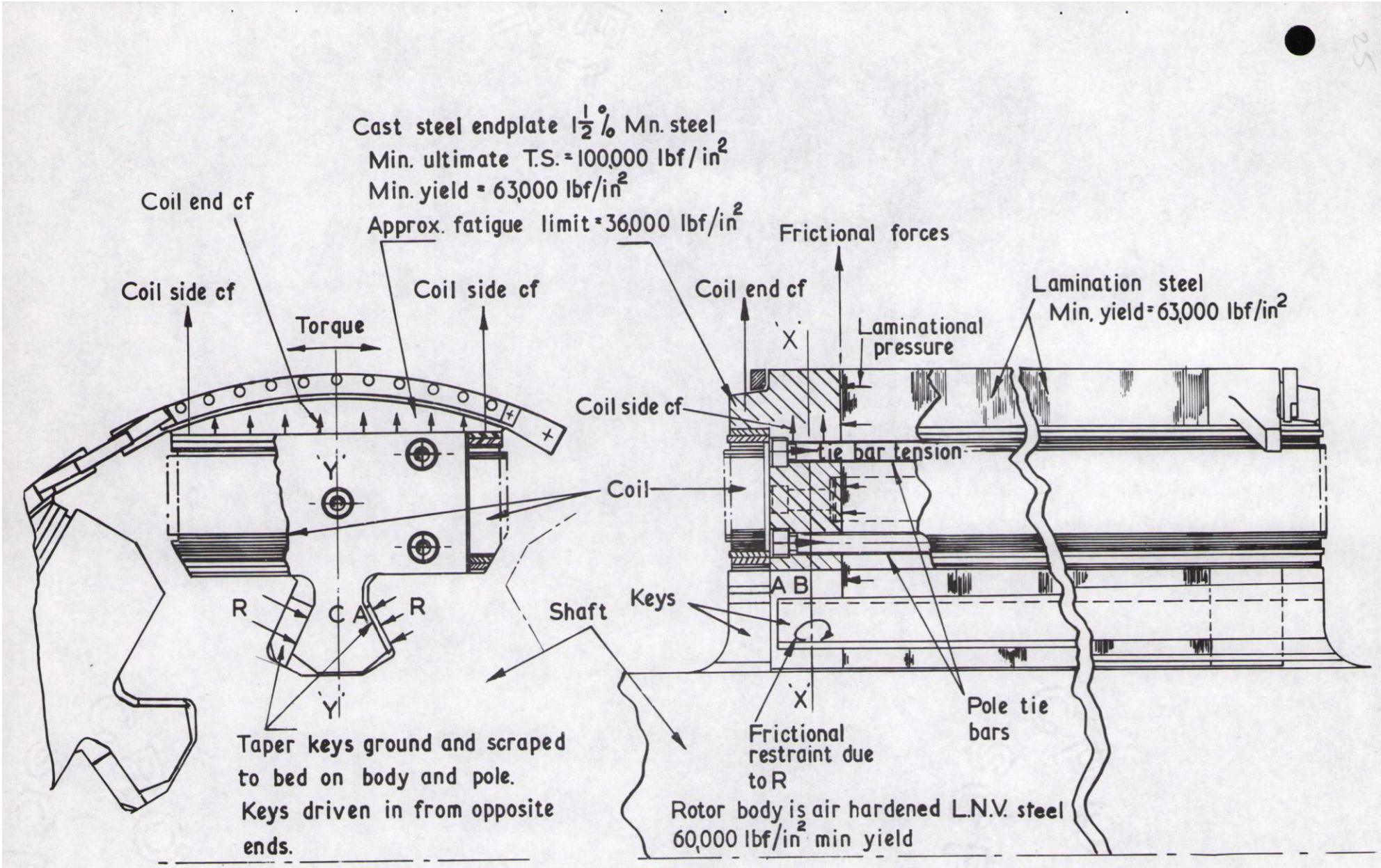

FIG. 5 ORIGINAL POLE CONSTRUCTION

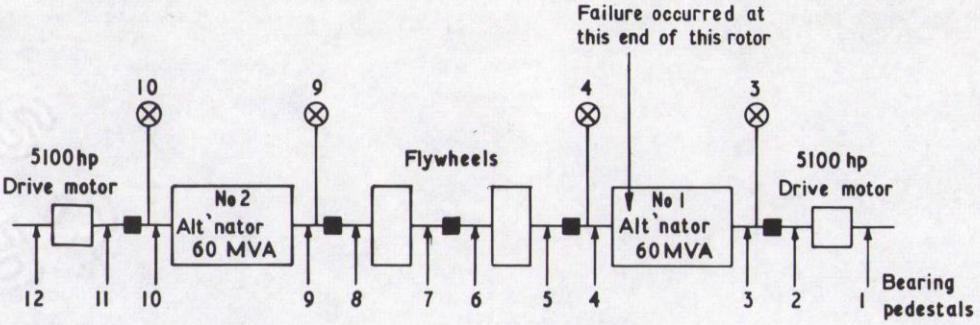

Vibration pick ups on all pedestals
Vibration recording equipment provided for pedestals 3,4,9 & 10
Eccentricity equipment installed at locations shown ⊗
Shaft system end to end approximately 100 feet long

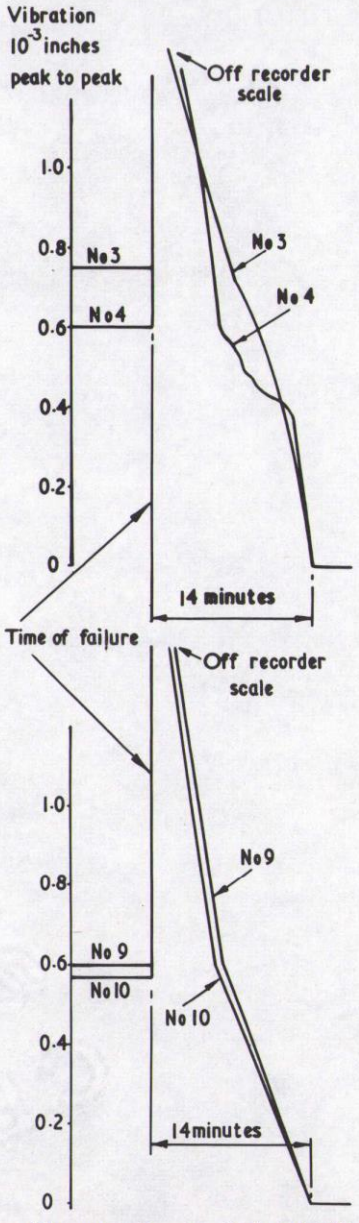

Alternator Bearing Pedestal Vibration Recordings At Time Of Failure

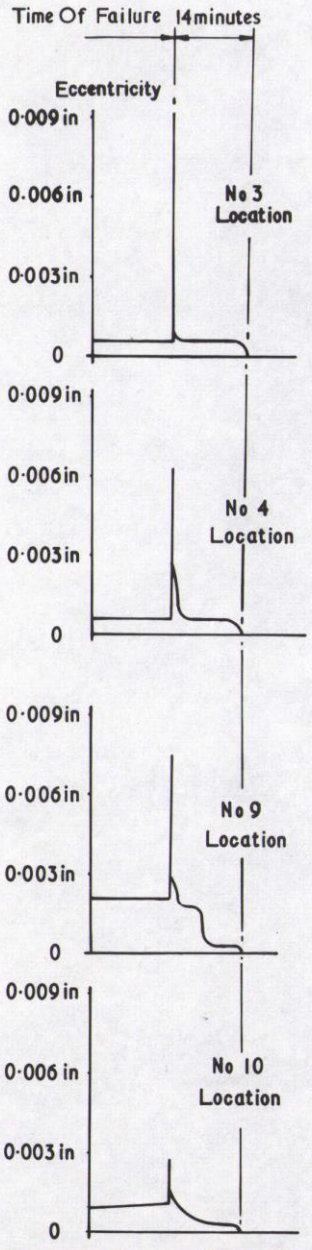

Alternator Shaft Eccentricity Recordings At Time Of Failure

FIG.6 SHAFT ECCENTRICITY & VIBRATION

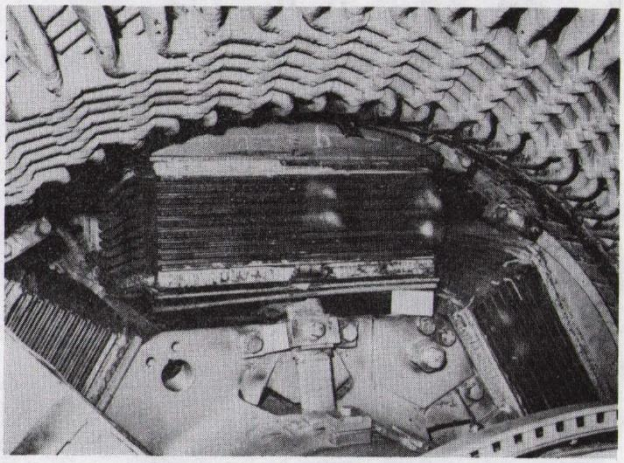

FIG. 7 DAMAGED POLE AND STATOR

FIG. 8 LOWER HALF OF FRACTURED DOVETAIL

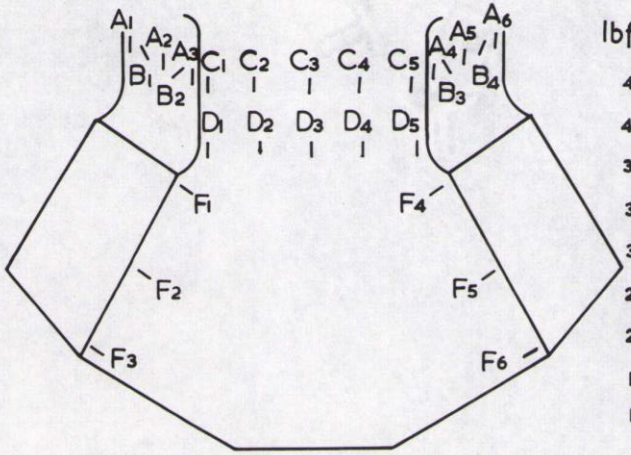

(a) Strain gauge layout

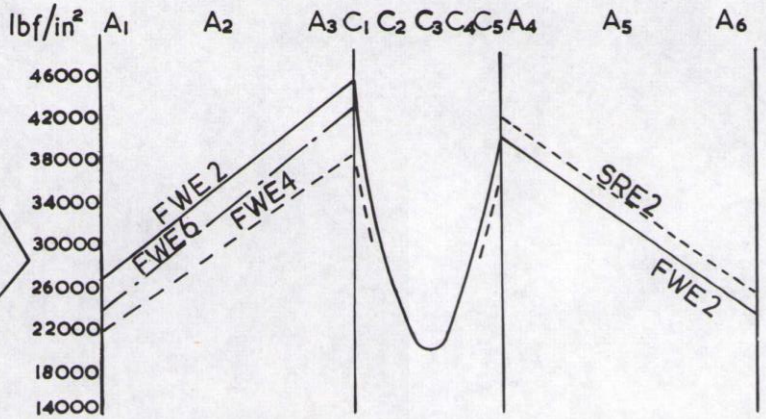

FWE – End of rotor adjacent to flywheel

SRE – Slip ring end of rotor

The figure denotes the pole number

(b) End Plate Stress Distribution (Set at speed but not pulsing)

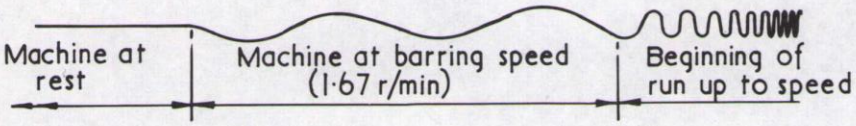

Part of high speed trace when machine is at full speed showing alternating component of stress of ±1450 lbf/in² at rotational frequency

(c) Gravitational component traces

FIG.9 STRAIN GAUGE LOCATIONS & MEASUREMENTS

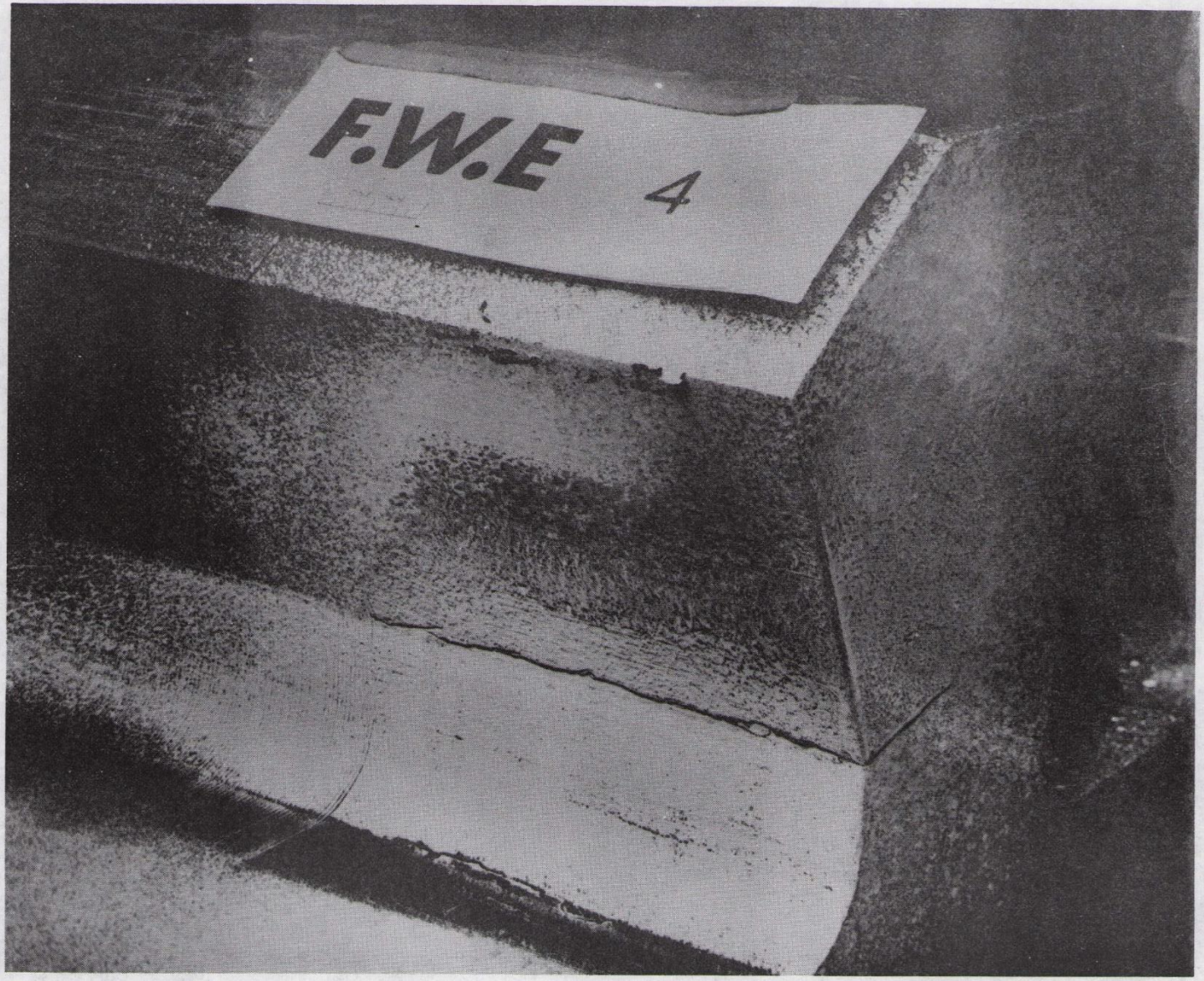

FIG.10 CRACKED ENDPLATE

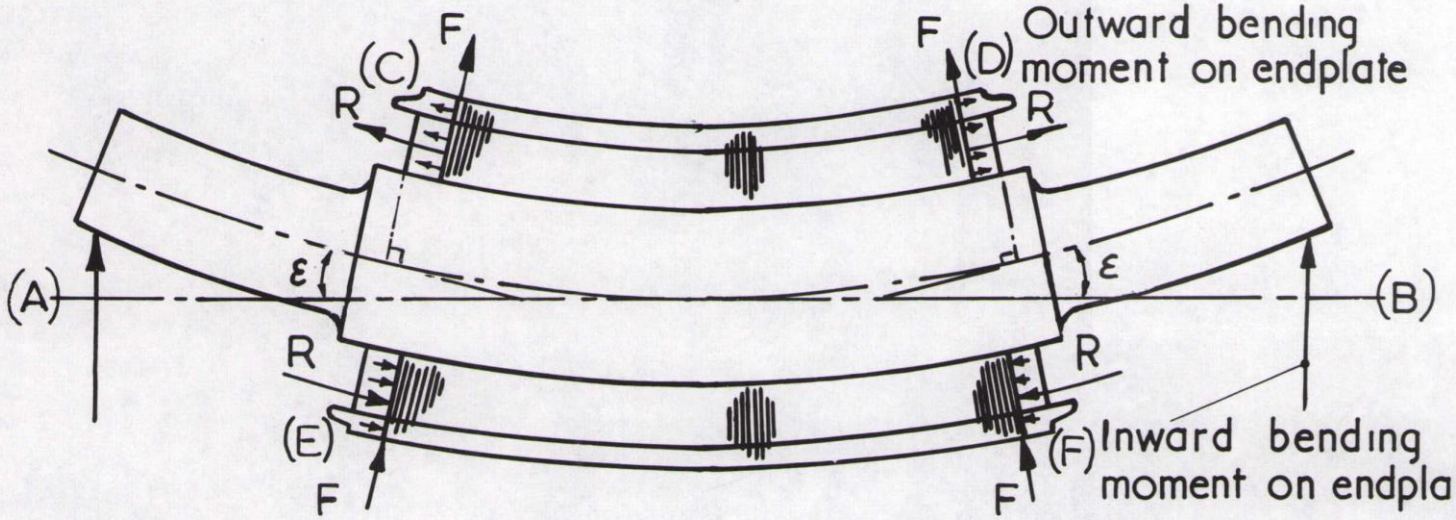

FIG.11 SHAFT STRESS CATENARY EFFECT

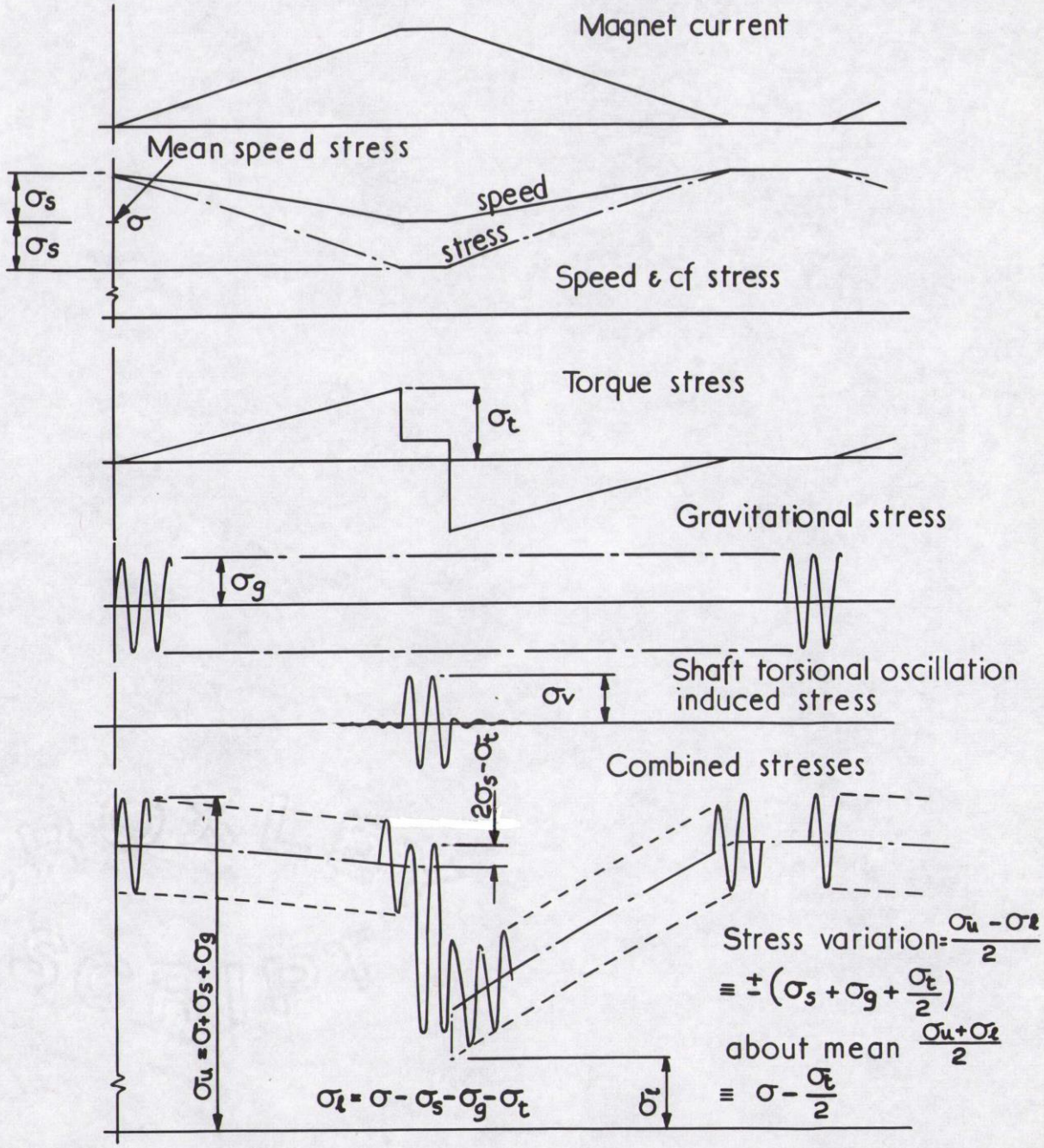

FIG.12 STRESS VARIATIONS (SIMPLIFIED) DURING PULSE

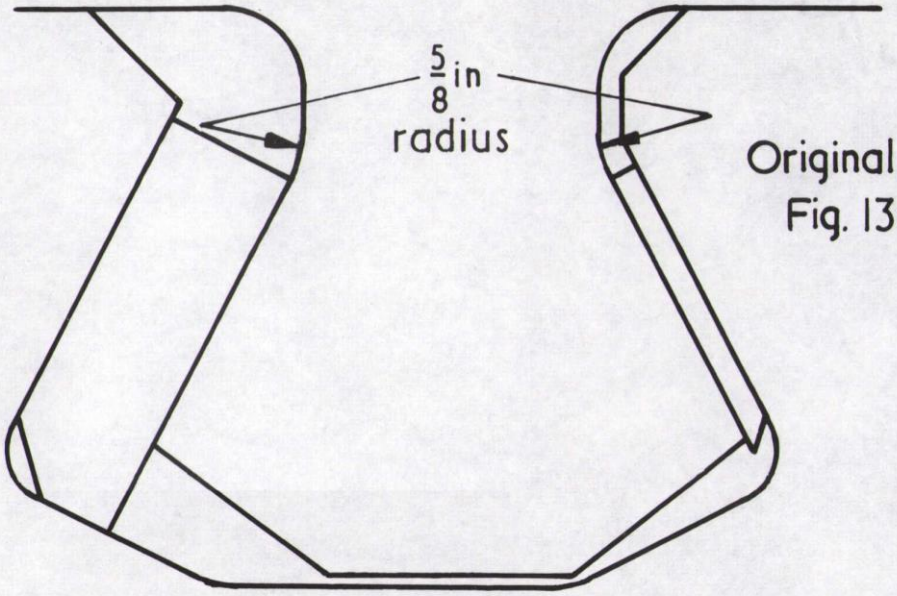

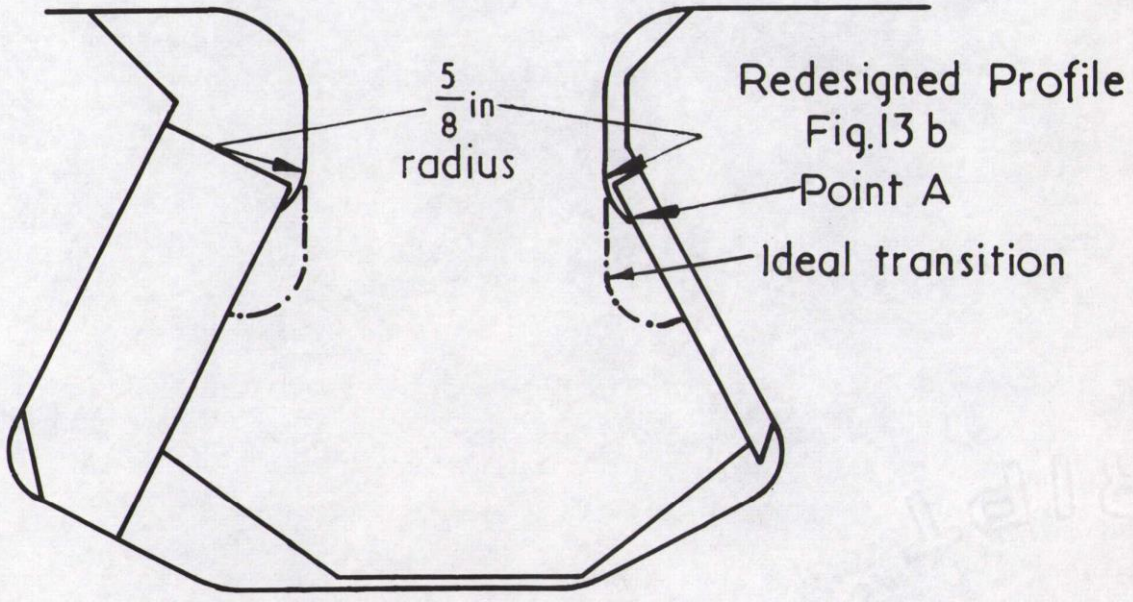

FIG. 13 POLE DOVETAIL PROFILES

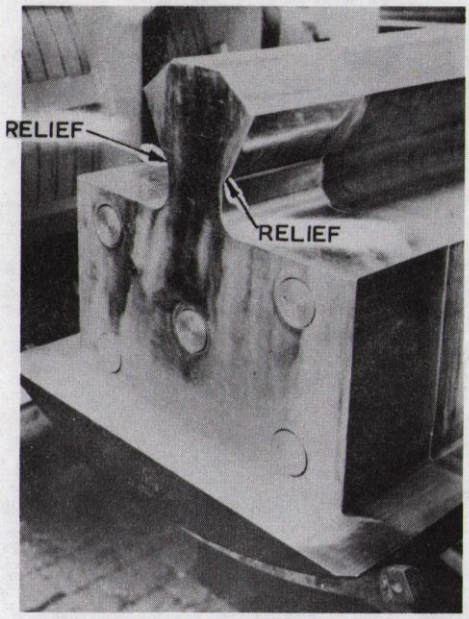

FIG. 14 PART OF REDESIGNED ENDPLATE POLE ASSEMBLY SHOWING RELIEFS

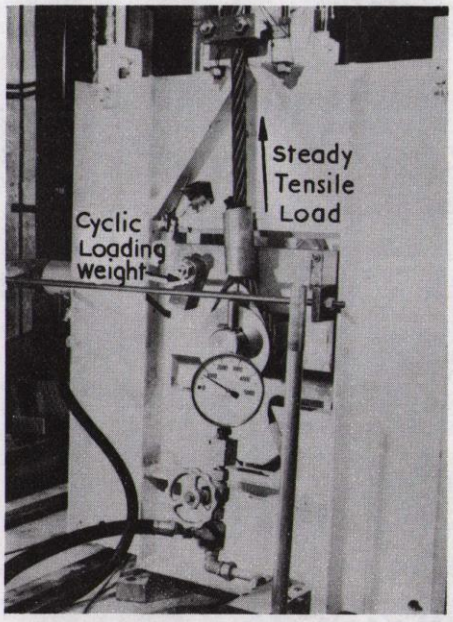

FIG. 15 ENDPLATE PROFILE AND MATERIAL TEST RIG

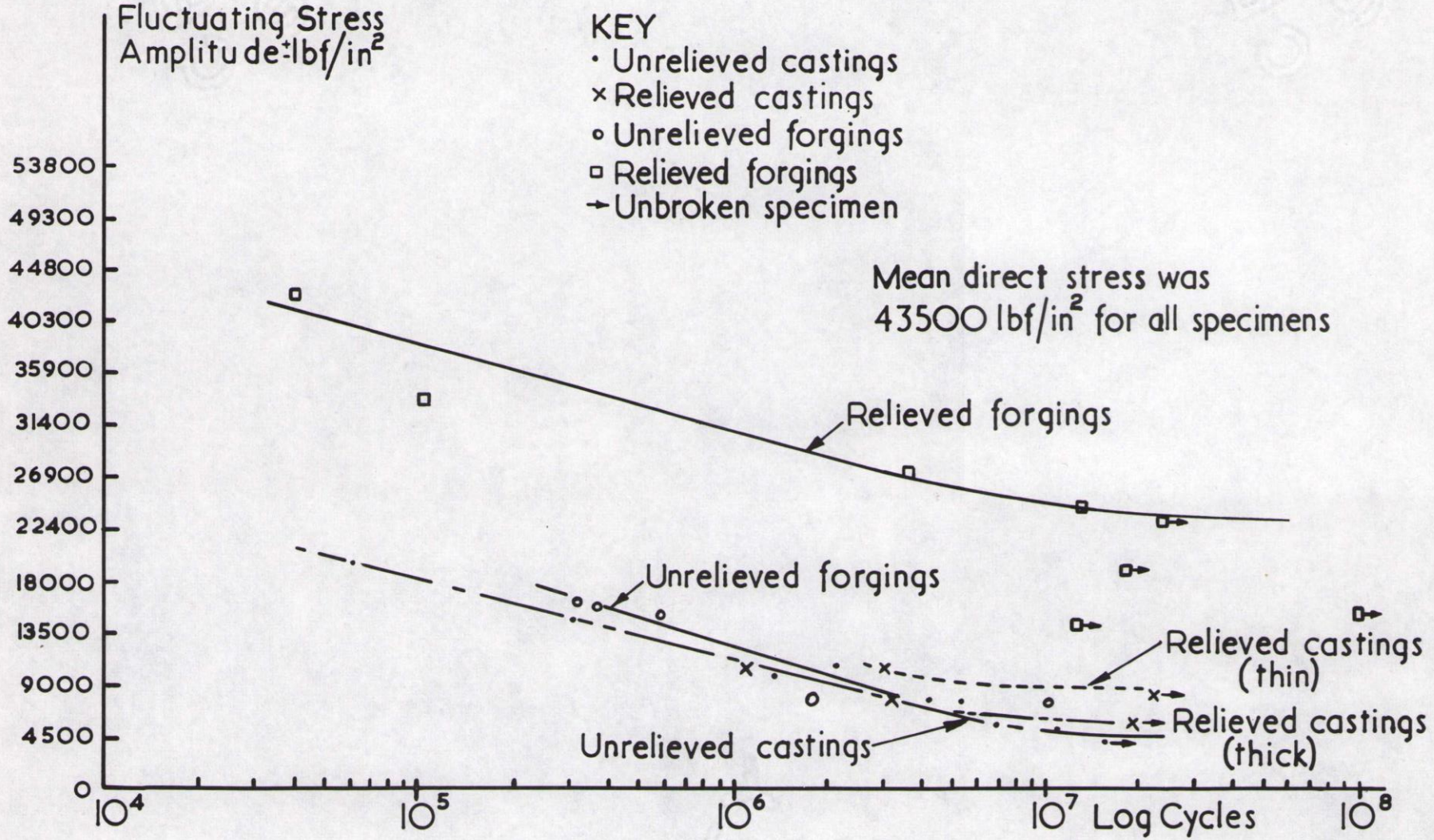

FIG. 16 FATIGUE CURVES OBTAINED FROM TEST RIG RESULTS

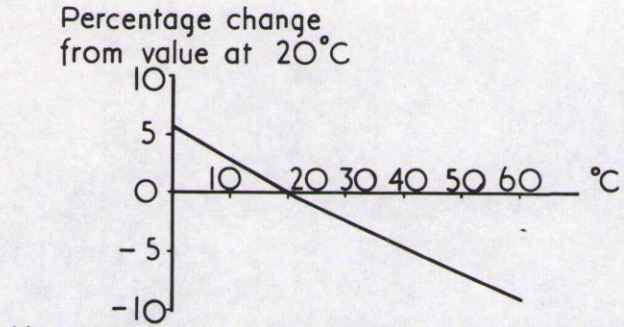

(a) EFFECT OF TEMPERATURE ON GAUGE FACTOR (P type gauge mounted on steel)

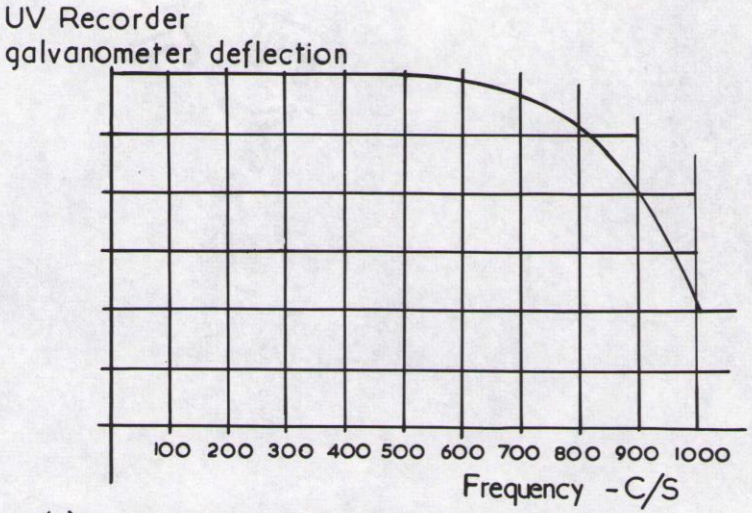

(b) OVERALL FREQUENCY RESPONSE OF STRESS MEASURING SYSTEM

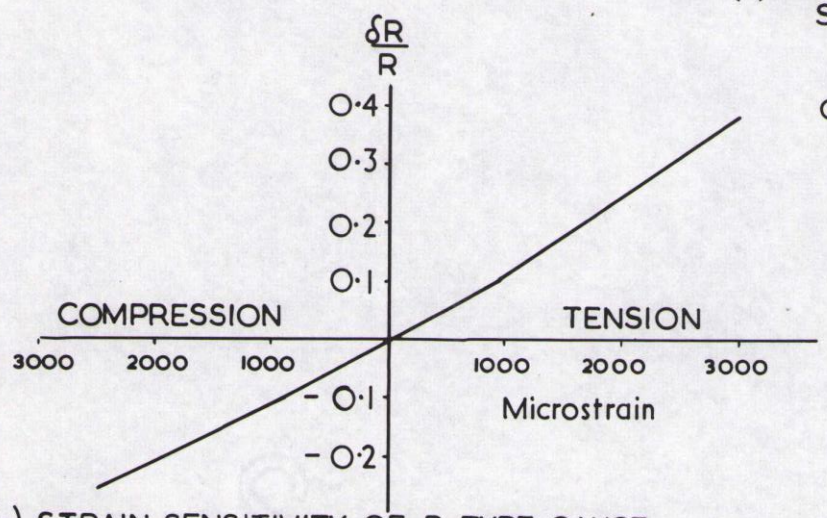

(c) STRAIN SENSITIVITY OF P TYPE GAUGE

$$\text{Gauge factor} = \frac{\frac{\delta R}{R}}{\frac{\delta L}{L}} = \frac{\delta R}{Re}$$

Where

R = Unstrained resistance of gauge

δR = Change in resistance due to L

δL = The increase or decrease in L

L = Original length

e = Mechanical strain

FIG.17 SILICON PIEZO RESISTIVE STRAIN GAUGE CHARACTERISTICS

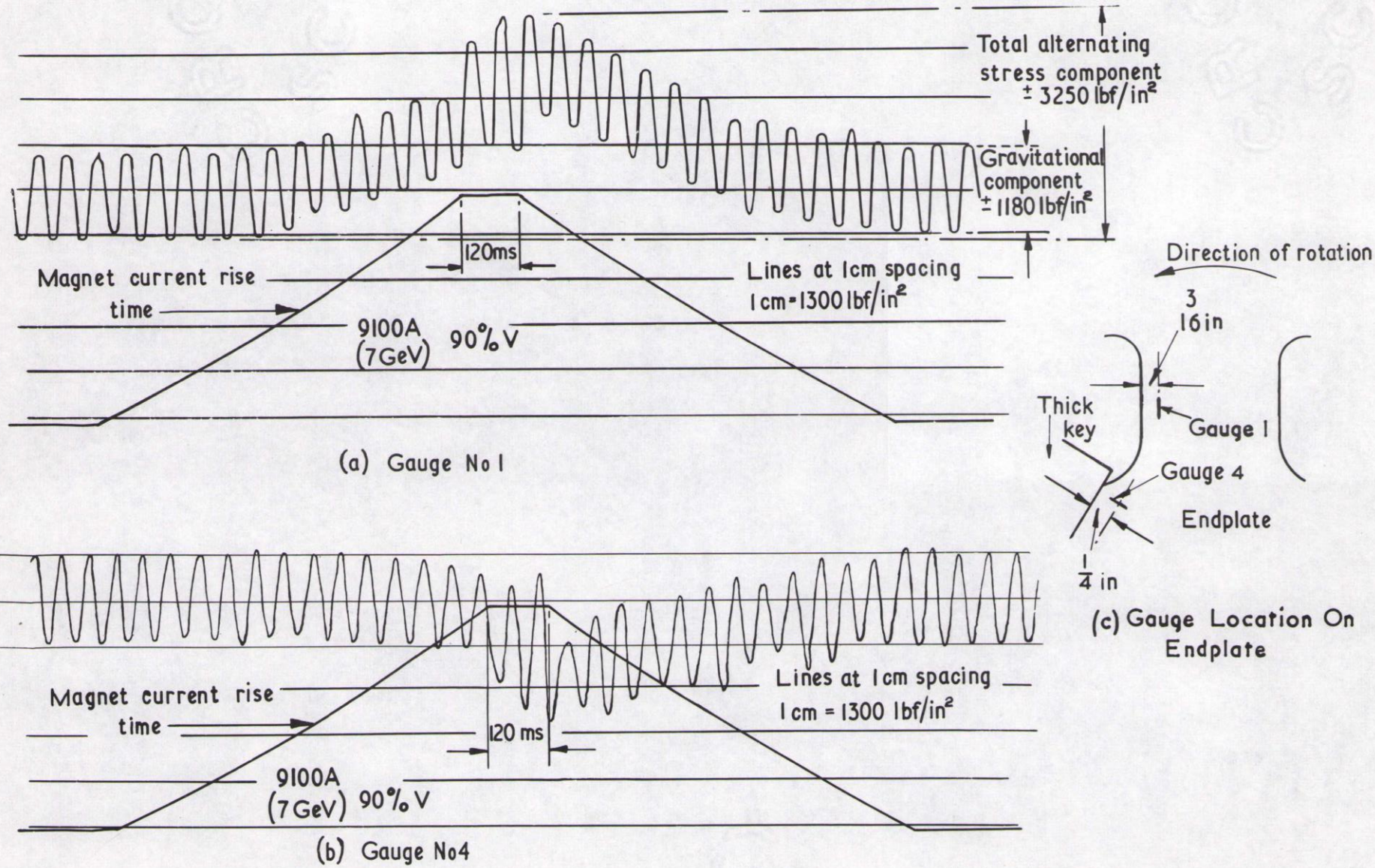

FIG.18 U.V. RECORDINGS OF CYCLIC STRESSES USING SILICON PIEZO RESISTIVE STRAIN GAUGES

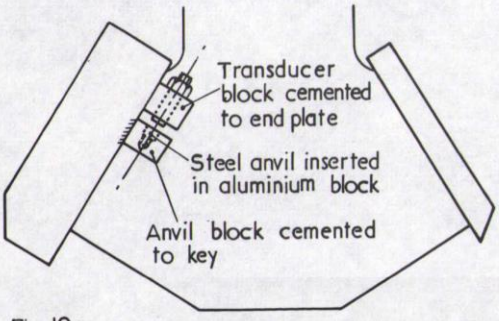

Fig. 19a
Arrangement Of Transducer And Anvil

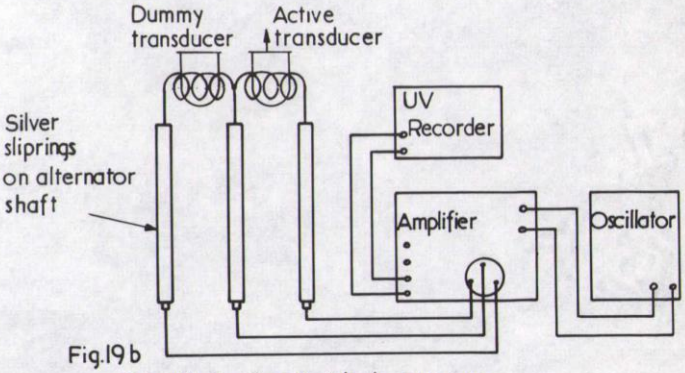

Fig.19b
Simplified Circuit Block Diagram

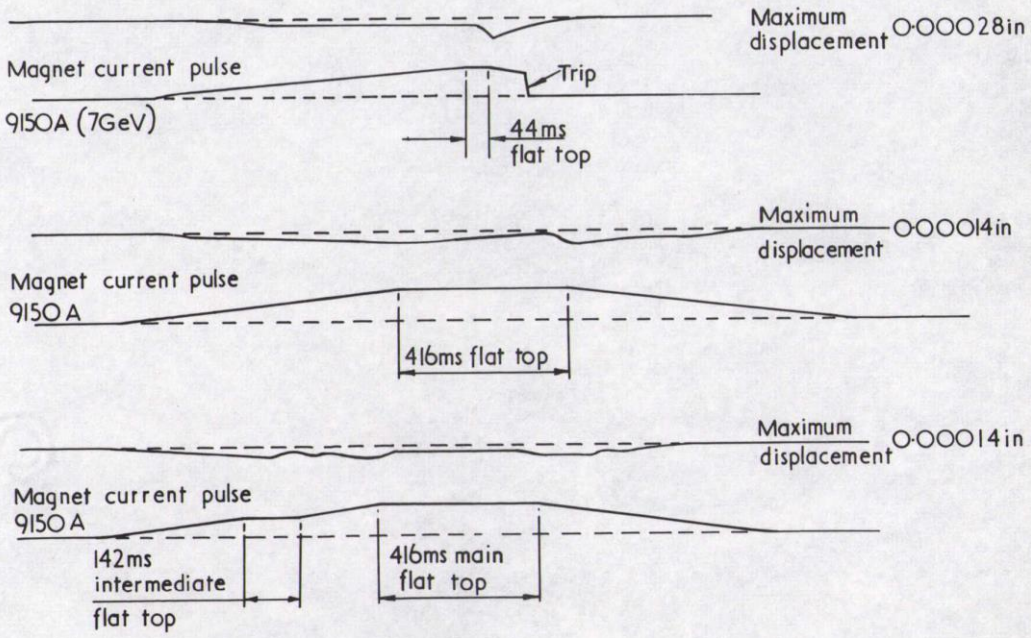

Fig.19c Typical Traces Of Key/Endplate Movement

FIG. 19 MEASUREMENT OF KEY/ENDPLATE MOVEMENT